Article

Journal of
Nanoscience and Nanotechnology
Vol. 15, 9281–9286, 2015
www.aspbs.com/jnn

Structural and Magnetic Characterizations of Nano Sized Grain Zinc Ferrite/Hydroxyapatite Ceramic Prepared by Solid State Reaction Route

Piyapong Pankaew[1,*] and Pattarinee Klumdoung[2]

[1] *Division of Industrial Materials Science, Faculty of Science and Technology, Rajamangala University of Technology Phra Nakhon, Bangkok 10800, Thailand*
[2] *Division of Physics, Department of Science, Faculty of Science and Technology, Rajamangala University of Technology Krungthep, Bangkok 10120, Thailand*

A promising composite of bioactive hydroxyapatite (HAp) and zinc ferrite ($ZnFe_2O_4$) has potentials for future bone reinforcing formation. In present study, HAp and $ZnFe_2O_4$ composite ceramic was prepared by solid state reaction route for easier control of structural and magnetic characteristics and with low cost. HAp powder was synthesized by precipitation method from chicken eggshell. Mixed powders with varying $ZnFe_2O_4$/HAp weight ratios from 2–10 wt% were milled together and uniaxially pressed and then sintered at 1200 °C for 3 hours. The XRD results showing no other phases of composite ceramics with only HAp and $ZnFe_2O_4$ phases were identified, indicating high stability of HAp property. Phase fractions of $ZnFe_2O_4$ were found to increase from 10.8 to 18.73 wt% with increasing content of $ZnFe_2O_4$. FT-IR results were only revealed vibration bands of standard HAp phase. SEM results revealed primary grains sizes of the prepared ceramics in nano scale. The BET surface area and pore volume increased with increasing content of $ZnFe_2O_4$ in composite ceramics. The VSM results of composites with increasing $ZnFe_2O_4$ content had been shown with increasing magnetization from 0.05 to 1.85 emu/g while their coercivities were decreased from 44 to 24 Oe. Higher magnetization as well as higher super paramagnetic behavior could be achieved with increasing the studied $ZnFe_2O_4$ weight ratios in $ZnFe_2O_4$/HAp composite ceramics, which can be tailored for specific applications.

Keywords: Hydroxyapatite, Zinc Ferrite, Composite Ceramic, Solid State Reaction Route.

1. INTRODUCTION

Magnetic therapy has been considered a promising alternative in disease treatments in health care, especially in the treatments of bone diseases. Hydroxyapatite (HAp, $Ca_{10}(PO_4)_6(OH)_2$) has been recognized as one of the most promising materials for hard tissue implants in orthopedic and dental surgeries due to its excellent biocompatibility and chemical similarity with bones and teeth.[1] Therefore composites of HAp and magnetic material with of unique magnetic property and biocompatible characterization have recently received great interests and widely developed in biomedical applications such as drug delivery materials, catalysts and hyperthermia agents. Previously, particle composites consisting of HAp and Fe_3O_4, γ-Fe_2O_3, $CoFe_2O_4$, $MnFe_2O_4$ or $MgFe_2O_4$ had been demonstrated by several techniques such as wet co-precipitation, hydrothermal method, ultrasonic spray pyrolysis, microwave irradiation, ultrasonic irradiation and mechanochemical route.[2–7] The preparation methods have some disadvantages such as the long reaction time requirement and subsequent heat treatment to the complete magnetic HAp crystallization and moreover its induction of other impurity phases which subsequently as a result reduces HAp stability. Recently, the materials have been actively studied for possibilities in bone tissue engineering applications by fabricating magnetic HAp scaffolds/substrates for bone regeneration.[8–11] However, the preparation of scaffolds/substrates for bone regeneration application has been rarely considered in comparison

*Author to whom correspondence should be addressed.

with the other forms of the composites for biomedical applications.

In this work; therefore, an easy method was proposed to produce a promising composite ceramic consisting of HAp and Zinc ferrite ($ZnFe_2O_4$) by using solid state reaction route. This method was expected to have better controllability of structural and magnetic characteristics and with commercial feasibility. The effect of $ZnFe_2O_4$ weight ratios on characteristics of the $ZnFe_2O_4$/HAp composite ceramics was investigated in a range from 2–10 wt%. Chicken eggshells were chosen to be calcium source for synthesizing HAp because they compose of high calcium content with low cost and can be easily procured.[12] Particularly, HAp synthesized from eggshells had significantly higher bone regeneration than commercial HAp at long time.[13] $ZnFe_2O_4$ was chosen as the magnetic component because previous reports have been demonstrated bone growth and bone mineralization can be stimulated by Zn. Moreover, it benefits for an antimicrobial action and also decreases the inflammatory reaction.[14,15] Thus $ZnFe_2O_4$ was not only expected to reveal magnetic behavior but also to accelerate bone formation for future implants. The prepared ceramic samples were characterized X-ray diffraction (XRD), Fourier transform infrared spectroscopy (FTIR), scanning electron microscopy (SEM), Brunauer-Emmett-Teller (BET) analyzer and vibrating sample magnetometer (VSM). These results will lead us to a methodology development for fabricating of $ZnFe_2O_4$/HAp composite ceramic optimized for specific applications.

2. EXPERIMENTAL DETAILS

2.1. HAp Preparation

In present work, hydroxyapatite (HAp) powders were prepared by precipitation reaction between $Ca(NO_3)_2$ solution prepared from chicken eggshells ($CaCO_3$) and $(NH_4)_2HPO_4$ solution with Ca/P mol concentration ratio of 1.67. Fresh chicken eggs as the starting source in preparing HAp were obtained from Charoen Pokphand Foods, (CPF) public company limited, Bangkok, Thailand. Membranes were removed and the eggshells were washed with distilled water to remove impurities and left in air to dry for a few days. Then, these shells were ground using an agate mortar to obtain fine ($CaCO_3$) powder. The theoretical reaction for preparing the HAp is given by equations:

$$CaCO_3 \rightarrow CaO + CO_2 \quad (1)$$

$$CaO + 2HNO_3 \rightarrow Ca(NO_3)_2 + H_2O \quad (2)$$

$$10Ca(NO_3)_2 + 6(NH_4)_3PO_4 + 2NH_4OH \rightarrow Ca_{10}(PO_4)_6(OH)_2 + 20NH_4NO_3 \quad (3)$$

Firstly sufficiently powdered eggshells were calcined at 1300 °C for 4 hours to acquire the 0.33 mole of CaO powders.[16] The prepared CaO powders were dissolved in 65% HNO_3 solution to make $Ca(NO_3)_2$ solution of 1 molar and adjusting pH to 10–12 with 30% NH_4OH solution. To prepare 0.6 molar of $(NH_4)_3PO_4$ solution, 0.2 mole of $(NH_4)_2HPO_4$ powders was dissolved in distilled water and pH was again adjusted to 10–12 with 30% NH_4OH solution. The prepared $(NH_4)_3PO_4$ solution was slowly added into continuously stirred $Ca(NO_3)_2$ solution for 4 hours. The suspensed particles were left at room temperature for 8 hours for complete reaction. Then the precipitated suspension was poured and filtrated and thoroughly washed with distilled water several times to remove excess ions. The cleaned precipitate was dried at 80 °C in an oven for 12 hours and finally ground using an agate mortar to obtain fine HAp powders.

2.2. $ZnFe_2O_4$ Preparation

ZnO and Fe_2O_3 powders were mixed with stoichiometry ratio of 1:1 in ethanol solution and introduced into a stainless steel vial with stainless steel balls in a high energy mixer/mill (SPEX-8000-D) for 10 minutes. Then the mixed powders were dried and ground before calcining at 1100 °C for 2 hours to complete the formation of $ZnFe_2O_4$.

2.3. $ZnFe_2O_4$/HAp Ceramic Preparation

Finally composite powders of $ZnFe_2O_4$ and HAp were introduced in a stainless steel vial containing stainless steel balls of diameter 10 mm with mixing mass ratio of powder/ball be 1:10 and were milled in a SPEX 8000-D mixer/mill for 10 minutes. Green compacts of these composites of five different amounts of $ZnFe_2O_4$ additions (2, 4, 6, 8 and 10 wt%) were prepared using a single-end die pressing. They were subsequently sintered at 1200 °C for 1 hour. The weight ratios of $ZnFe_2O_4$ to HAp investigated in this work were 2/98, 4/96, 6/94, 8/92 and 10/90, respectively. The composite ceramic 2/98 represents the composite ceramic containing 2% of $ZnFe_2O_4$ and 98% of HAp by weight.

2.4. Sample Characterization

The crystal structure of samples was identified by an X-ray diffractometer (XRD model-PW-1830). These analyses were carried out on powder samples with a Philips diffractometer using monochromatized CuK_α radiation. The X-ray tube was operated at 30 kV and 25 mA. The samples were scanned in the 2θ range of 20°–60° with a step of 0.02° and a scanning time of 8 seconds. The function groups of the prepared ceramics were analyzed by fourier transform infrared-attenuated total reflectance (FTIR-ATR) spectroscopy technique. All FT-IR measurements were carried at room temperature over the range from 515–2000 cm^{-1} using a FT-IR spectrometer (Perkin Elmer model 2000). The morphology of the samples was examined using a scanning electron microscope (SEM, Hitachi, S-4700) operated at 10 kV. The specific surface

area and pore volume of specimens were made by BET surface area analyzer (Quantachrome model: Autosorb-1) using nitrogen adsorption at 77 K. The magnetic properties were made by vibrating sample magnetometer (VSM). The hysteresis loops were recorded at room temperature with maximum applied field up to 9000 Oe.

3. RESULTS AND DISCUSSION

X-ray diffraction patterns of the prepared HAp, $ZnFe_2O_4$ and $ZnFe_2O_4$/HAp composite ceramics are shown in Figure 1. The dominant diffraction peaks of HAp corresponded to the (002), (102), (201), (211), (112), (300), (202), (130), (222), (312), (213), (321), (140), (402) and (004) planes of hexagonal symmetry in the JCPDS file number 74-0566. The diffraction peaks of $ZnFe_2O_4$ phase were indexed to the crystal planes of cubic spinel $ZnFe_2O_4$ according to the JCPDS file number 82-1049. The biphasic phases consisting of only the HAp and the $ZnFe_2O_4$ phases were observed for all conditions, indicating no phase transformation. The $ZnFe_2O_4$ phase was only observed at (311) plane. The XRD patterns of composite ceramics showed well matching of peak positions and intensities with those of the standard HAp phase. Similar results were also reported by other researchers which demonstrated the magnetite particle is well functionalized in the hexagonal structure of HAp without disturbing calcium phosphate crystal lattice.[6, 10]

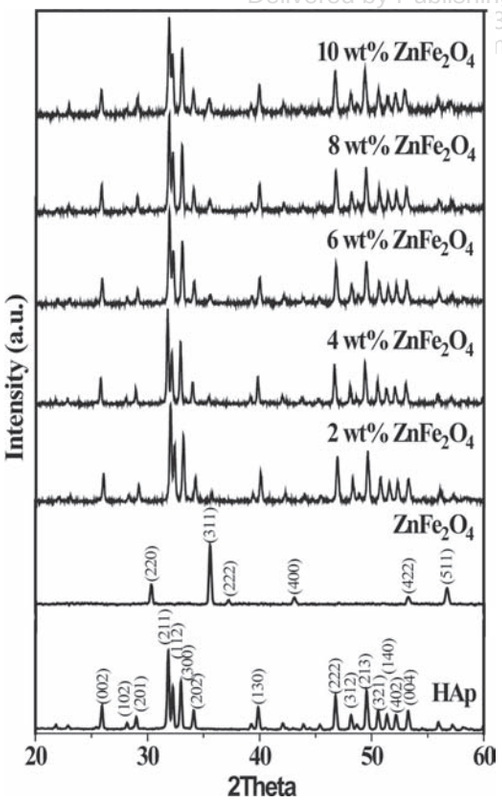

Figure 1. X-ray diffraction patterns of HAp, $ZnFe_2O_4$ and $ZnFe_2O_4$/HAp composite with five different $ZnFe_2O_4$ contents.

To further confirm the stability of HAp structure in composite ceramics, the lattice parameter and the crystallite size of $ZnFe_2O_4$ and HAp phases in composite phases are reported in Table I. The lattice parameters of HAp phase in composite ceramics were in the range of $a = 0.9350$–0.9407 nm and $c = 0.6837$–0.6896 nm, close to pure HAp phase ($a = 0.9418$ nm and $c = 0.6884$ nm). There was insignificant relevance between both lattice parameters of HAp and $ZnFe_2O_4$ phases as increased $ZnFe_2O_4$ weight ratios in composite. However, lattice parameter variation of HAp directly related to that of $ZnFe_2O_4$ indicating the interaction between $ZnFe_2O_4$ and HAp phases. The average crystallite sizes of HAp and $ZnFe_2O_4$ in composite ceramics, qualitatively calculated from the FWHM of the HAp (002) plane and the $ZnFe_2O_4$ (311) plane using Scherrer's formula, were found to be in the range of 60.02–63.05 nm and 45.76–81.38 nm, respectively. The HAp crystal from our results had been shown with small crystal size which exhibiting a higher bioactivity in comparison to coarse crystals. Moreover, the finer crystals also provide larger interfaces for osseointegration.[17, 18]

For $ZnFe_2O_4$/HAp phase composition, it was found the intensity height of $ZnFe_2O_4$ peak was related directly to the $ZnFe_2O_4$ weight ratio. $ZnFe_2O_4$ phase fractions in composite ceramics were found to be 10.81, 11.15, 14.05, 16.18 and 18.73 wt% when $ZnFe_2O_4$ weight ratios were increased from 2 to 10 wt%, respectively, as shown in Table I. The remaining high HAp phase fraction in composite ceramic indicated the high stability of HAp property. From overall results, it can conclude that solid state reaction method consisting of mechanical milling and sintering process could be used to fabricate the $ZnFe_2O_4$/HAp composite ceramics with no induction of any phases and no change of HAp structure after the functionalization with magnetic particle indicating high stability of HAp property. It is noted that the $ZnFe_2O_4$/HAp phase composition could be clearly controlled by changing the $ZnFe_2O_4$ weight ratios of composite ceramics.

The chemical structure and functional groups of $ZnFe_2O_4$/HAp composite ceramic with different weight ratios investigated using FT-IR (ATR) spectroscopy are shown in Figure 2. From the results, no $ZnFe_2O_4$ band could be observed in the spectrum. This may due to the overlapping of the $ZnFe_2O_4$ vibrational bands with HAp bands. However, their intense variations observed in HAp vibrational bands indicated the interaction between $ZnFe_2O_4$ and HAp. In HAp bands, the broad bands of –OH groups are presented around 632 cm^{-1}. The broadband observed at about 960 cm^{-1} corresponds to υ_1 symmetric P–O stretching vibration of the PO_4^{3-}. The band between 570 and 600 cm^{-1} is referred to υ_4 vibration mode of PO_4^{3-} group occupying two sites in the crystal lattice. A major peak at 1092 cm^{-1} of PO_4^{3-} is identified as the υ_3 vibration band, which is the most intensified peak among the

Table I. The phase fraction, lattice parameter and the crystallite size of $ZnFe_2O_4$ and HAp phases in composite phases.

	HAp phase				$ZnFe_2O_4$ phase		
		Lattice (nm)					
wt% $ZnFe_2O_4$	% Phase fraction	*a*	*c*	Crystallite size (nm)	% Phase fraction	Lattice *a* (nm)	Crystallite size (nm)
2	89.19	0.9350	0.6837	60.02	10.81	0.8328	81.38
4	88.85	0.9407	0.6896	62.64	11.15	0.8392	74.69
6	85.95	0.9372	0.6869	61.54	14.05	0.8362	55.31
8	83.82	0.9384	0.6880	63.05	16.18	0.8382	53.61
10	82.27	0.9373	0.6880	60.55	17.73	0.8387	45.76

phosphate vibration modes. The band at 1366–1370 cm^{-1} corresponds to υ_3 asymmetric stretching of the C–O bond of CO_3^{2-} in both A- and B-type substitutions in HAp lattice. $P_2O_7^{4-}$ group at 1216 is observed. A peak appeared at 1732–1736 cm^{-1} attributes the combination of υ_1 asymmetric stretching and υ_4 bending of CO_3^{2-} group. With an increase in $ZnFe_2O_4$ weight ratios, there was a decrease in the intensity of these bands. Adding the $ZnFe_2O_4$ in composite may inhibit these ion substitutions in HAp lattice resulting on the decreased intensity of these group bands. The shape of FT-IR spectra for the composite ceramics of all weight ratios had been shown in similar pattern.

The hysteresis loops of the $ZnFe_2O_4$/HAp composite ceramics with five different $ZnFe_2O_4$ contents are shown in Figure 3. The saturation magnetizations (M_s) of composite ceramic were found to be 0.05, 0.36, 0.76, 1.21, and 1.85 emu/g, while their coercivities were found to be 44.00, 36.16, 34.40, 29.20, and 24.14 Oe with the increasing of $ZnFe_2O_4$ weight ratios from 2 to 10 wt%, respectively. The increased M_s could be attributed to the enhancement of the total magnetic moments, which result from the increase of $ZnFe_2O_4$ weight in composite ceramics. Moreover the results confirmed the superparamagnetic behavior of these composite ceramics, indicated by a low coercivity value.

Thus it can conclude that the increasing of $ZnFe_2O_4$ in $ZnFe_2O_4$/HAp composite ceramics primarily resulted in higher saturation magnetization and higher superparamagnetic behavior. The M_s value of $ZnFe_2O_4$/HAp composite ceramics was close to that of magnetic HAp previously reported.[10] It has been demonstrated that the magnetic HAp scaffold with low saturation magnetization could better stimulate cell adhesion, proliferation, and differentiation compared with the HAp scaffold due to the intrinsic magnetic field provided by the incorporated magnetic particles. Moreover these scaffolds well responded external magnetic field.[13] Therefore, $ZnFe_2O_4$/HAp composite ceramics with low magnetization obtained from our result is expected to be efficient in the future bone tissue regeneration application.

SEM images of the $ZnFe_2O_4$/HAp composite ceramics with five different amounts of $ZnFe_2O_4$ are shown in Figure 4. The grain morphology of these composite ceramics was observed to be in polygonal shapes. The primary grain sizes of composite ceramics in the range of nano scale were observed and tended to reduce from 850 nm to 620 nm with the increasing $ZnFe_2O_4$ weight ratios from 2 to 10 wt%, respectively. Moreover these composite

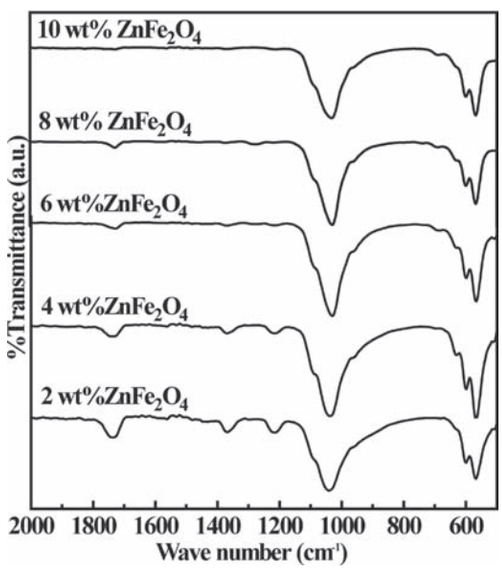

Figure 2. FT-IR (ATR) spectra of $ZnFe_2O_4$/HAp composite with five different $ZnFe_2O_4$ contents.

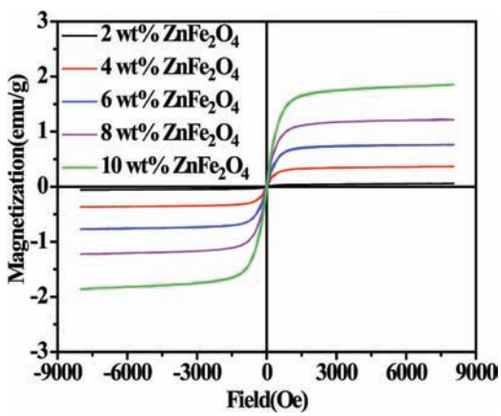

Figure 3. VSM of $ZnFe_2O_4$/HAp composite with five different $ZnFe_2O_4$ contents.

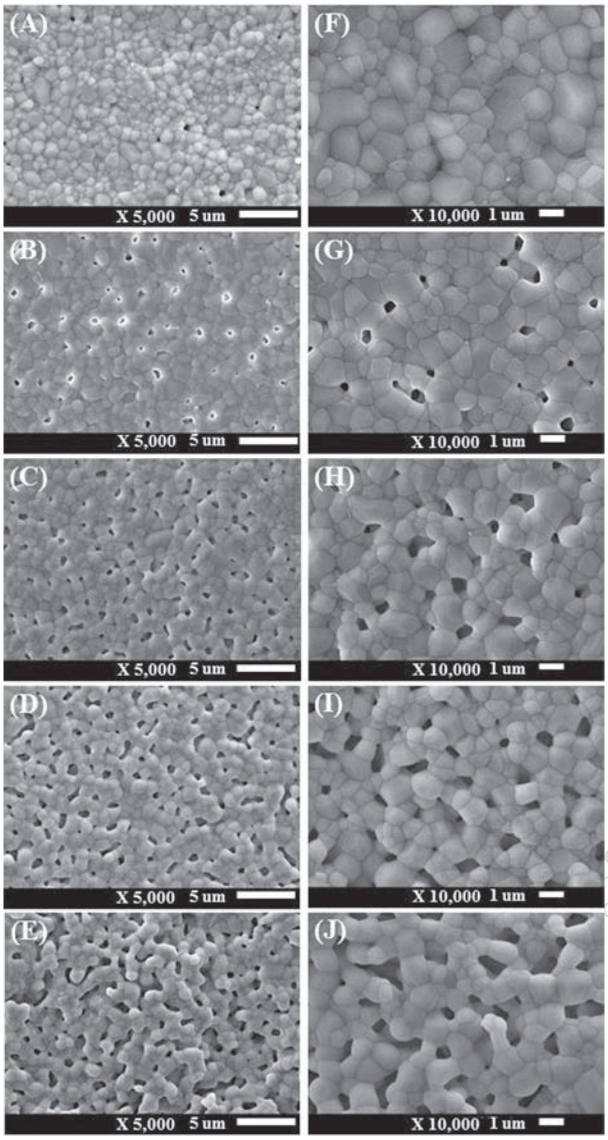

Figure 4. SEM images of $ZnFe_2O_4$/HAp ceramic with $ZnFe_2O_4$ amounts of (A), (F) 2 wt%, (B), (G) 4 wt%, (C), (H) 6 wt%, (D), (I) 8 wt%, and (E), (J) 10 wt%, at magnification × 5000 and × 10000, respectively.

ceramics exhibited an enhanced porosity and good interconnectivity with the increase of $ZnFe_2O_4$ weight ratios.

The significant change in porosity could be contributed to lower sinterability of the composite ceramic as increased $ZnFe_2O_4$ weight ratios in them. Also, micropores generated throughout structures will make them easy to get in touch with the organic components such as collagen, hyaluronic acid or surface modified groups when used as biomaterials. The BET surface area and pore volumes of these composites were measured to support SEM results as shown in Table II. The BET surface area and pore volume of composite ceramics were tended to increase from 0.67 to 15.35 m^2/g and 0.005 to 0.032 cc/g with the increasing $ZnFe_2O_4$ weight ratios, respectively. From overall results,

Table II. The BET surface area and pore volumes of $ZnFe_2O_4$/HAp composite ceramics.

wt% $ZnFe_2O_4$	Surface area (m^2/g)	Pore volume (cc/g)
2	0.67	0.005
4	2.47	0.007
6	8.63	0.018
8	9.74	0.030
10	15.35	0.032

it can be concluded that the surface morphology with nano grain size and high pore structure was observed with high surface area for cell attachment, indicative of good cell growth and differentiation.[19]

4. CONCLUSION

In the present work, a promising $ZnFe_2O_4$/HAp composite ceramic had been successfully prepared by solid state reaction route with intended application in the future bone reinforcing formation. The $ZnFe_2O_4$/HAp composite ceramic fabricated by this method was found no induction of any phases and no change of HAp structure after the functionalization with magnetic particle indicating high HAp stability. The $ZnFe_2O_4$/HAp phase composition could be clearly controlled by changing the $ZnFe_2O_4$ weight ratios in composite ceramics. The higher saturation magnetization as well as higher super paramagnetic behavior could be easily altered by increasing $ZnFe_2O_4$ content in the composite ceramic. The surface morphology of these composite ceramics exhibited primary grain in nano scale with enhanced pore structure when $ZnFe_2O_4$ weight ratios increased; indicating high surface area for cell attachment and better cell growth and differentiation. Therefore, the results confirmed $ZnFe_2O_4$/HAp composite ceramic prepared by this method is expected with good potential and efficient for the future bone regeneration application.

Acknowledgment: We would like to thanks the Department of Chemistry, Faculty of Science, King Mongkut's Institute of Technology Ladkrabang for providing BET analysis. This research was financially supported by Faculty of Science and Technology, Rajamangala University of Technology Phra Nakhon (RMUTP).

References and Notes

1. S. V. Dorozhkin, *Acta Biomater.* 6, 715 (**2010**).
2. N. Petchsang, W. P. On, J. H. Hodak, and I. M. Tang, *J. Magn. Magn. Mater.* 321, 1990 (**2009**).
3. A. Inukai, N. Sakamoto, H. Aono, O. Sakurai, K. Shinozaki, H. Suzuki, and N. Wakiya, *J. Magn. Magn. Mater.* 323, 965 (**2011**).
4. K. H. Zuo, Y. P. Zeng, and D. Jiang, *J. Nanosci. Nanotechnol.* 12, 7096 (**2012**).
5. H. Jiang, Y. Li, Y. Zuo, W. Yang, L. Zhang, J. Li, L. Wang, Q. Zou, L. Cheng, and J. Li, *J. Nanosci. Nanotechnol.* 9, 6844 (**2009**).
6. D. Gopi, M. Thameem Ansaria, E. Shinyjoy, and L. Kavitha, *Spectrochim. Acta A* 87, 245 (**2012**).

7. T. Iwasaki, R. Nakatsuka, K. Murase, H. Takata, H. Nakamura, and S. Watano, *Int. J. Mol. Sci*. 14, 9365 **(2013)**.

8. S. Panseri, C. Cunha, T. D'Alessandro, M. Sandri, A. Russo, G. Giavaresi, M. Marcacci, C. T. Hung, and A. Tampieri, *PLoS One* 7, e38710 **(2012)**.

9. S. Panseri, A. Russo, G. Giavaresi, M. Sartori, F. Veronesi, M. Fini, D. M. Salter, A. Ortolani, A. Strazzari, A. Visani, C. Dionigi, N. Bock, M. Sandri, A. Tampieri, and M. Marcacci, *J. Biomed. Mater. Res. A* 100A, 2278 **(2012)**.

10. X. B. Zeng, H. Hu, L. Q. Xie, F. Lan, W. Jiang, Y. Wu, and Z. W. Gu, *Int. J. Nanomed.* 7, 3365 **(2012)**.

11. A. Tampieri, T. D'Alessandro, and M. Sandri, *Acta Biomater.* 8, 843 **(2012)**.

12. D. L. Goloshchapov, V. M. Kashkarov, N. A. Rumyantseva, P. V. Seredin, A. S. Lenshin, B. L. Agapov, and E. P. Domashevskaya, *Ceram. Int*. 39, 4539 **(2013)**.

13. S. W. Lee, S. G. Kim, C. Balázsi, W. S. Chae, and H. O. Lee, *Oral Surg Oral Med Oral Pathol Oral Radiol Endod.* 113, 348 **(2012)**.

14. L. A. Grandjean, P. Laquerriere, E. Jallot, J. M. Nedelec, and T. M. Philips, *Biomaterials* 27, 3195 **(2006)**.

15. M. M. Rashad and M. I. Nasr, *Electron. Mater. Lett.* 8, 325 **(2012)**.

16. P. Pankaew, P. Klumdoung, E. Hoonnivathana, P. Limsuwan, and K. Naemchanthara, *Adv. Sci. Lett*. 19, 976 **(2013)**.

17. R. Murugan and S. Ramakrishna, *J. Cryst. Growth* 274, 209 **(2005)**.

18. J. Brandt, S. Henning, G. Michler, W. Hein, A. Bernstein, and M. Schulz, *J. Mater. Sci. Mater. Med*. 21, 283 **(2010)**.

19. I. O. Smith, L. R. McCabe, and M. J. Baumann, *Int. J. Nanomedicine* 1, 89 **(2006)**.

Received: 15 November 2014. Accepted: 27 January 2015.